A Robust Dual Mode Tilt Derivative-Integral Derivative Controller for Frequency Control Considering Renewable Energy Sources and Electrical Vehicle

R. Ramar *, M. Mohamed Thameem Ansari **, J. Raja ***, A.P. Srivishnupriya ****‡

**Department of Electrical Engineering, Faculty of Engineering and Technology, Annamalai University, Annamalai Nagar, Tamilnadu, India-608002.

** Department of Electrical Engineering, Faculty of Engineering and Technology, Annamalai University, Annamalai Nagar, Tamilnadu, India-608002.

*** Assistant Director, National Power Training Institute, Neyveli, India.

**** Department of Electrical and Electronics Engineering Assistant Professor, Krishnasamy College of Engineering and Technology, Cuddalore, Tamil Nadu, India

(ramar.nptisr@yahoo.com, ansariaueee@gmail.com, jrajaj1980@gmail.com, vishnuap28@gmail.com)

‡ Corresponding Author; A.P. Srivishnupriya, Postal address, Tel: +91 9442179013, vishnuap28@gmail.com

Received: 15.12.2023 Accepted:13.01.2024

Abstract -The uncertain renewable energy sources (RES) and electric vehicles (EVs) are being incorporated into the interconnected power system more and more these days. Additionally, there is also a sudden change in the load, which causes an undesirable deviation in the frequency range, which leads to the instable operation of the power system. To overcome the frequency regulation problem, automatic generation controllers (AGCs) such as integral (I), proportional (P), and proportional integral derivative (PID) are implemented. With these conventional AGC, it is not sufficient to handle the system with more integrated RES and EVs. To tackle this limitation, in this paper, a significant and simple Dual Mode Tilt Derivative and Integral Derivative Controller (DM TD-ID) is proposed and implemented for a complex Three Area Interconnected Power System (TAIPS), considering RES and EVs. The controller parameters are tuned with the use of a powerful JAYA optimization algorithm and the Integral Square Error (ISE) criterion for 1% of step load perturbation and to verify the efficiency of the proposed controller, it is compared with other conventional-type controllers such as P, PI, PID, and Tilt Integral Derivative (TID) controllers. According to the findings, the proposed JAYA-tuned DM TD-ID controller is determined to be more effective when compared to other conventional controllers. Also, different scenarios, including sensitivity analysis and performance analysis, are conducted to demonstrate the viability of the proposed controller for the TAIPS.

Keywords Automatic Generation Control, Dual Mode Tilt Derivative -Integral Derivative controller, Electrical Vehicle, Renewable Energy Sources, Frequency Regulation.

NOTATION	
ACE	Area Control Error
AGC	Automatic Generation Control
ISE	Integral Square Error
EV	Electric Vehicle
LFC	Load Frequency Control
TAIPS	Three Area Integrated Power System

SLP	Step Load Disturbance
HVDC	High Voltage Direct Current
$\Delta P_{Solar\ PV}$, ΔP_{WP}, (ΔG_{HY1}, ΔG_{HY2}),	Change in power output from Solar PV, wind power, Change in Hydro power generation.
ΔG_{TH},ΔG_{PS}	Change in Thermal power generation, Power System
ΔP_{G1},ΔP_{G2}, ΔP_{G3}	Change in generation in area1, area2 and area3
PID	Proportional Integral Derivative controller,
TID	Tilt Integral Derivative controller,
DM TD-ID	Dual-Mode Tilt Derivative and Integral Derivative Controller
ΔF_1, ΔF_2, ΔF_3	Frequency deviation in area1, area2, area3
ΔT_1, ΔT_2, ΔT_3	Power deviation in tie-line1, tie-line2, tie-line3.
U_E, T_E	AGC signal to EV and time constant of EV
B_i	Biasing coefficient in each area
ε	Switching limit
U(t)	Controller output signal
E(t)	Error signal into controller
$\Delta P_{tie\text{-}linej}$	Tieline power in j^{th} area
U(t)	controller output
E(t)	error signal
λ_i	fractional operator

1. Introduction

Nowadays, the demand for electricity is steadily increasing as a result of global population growth, industrialization, and improvements in living standards. Although combustion engines driven by fossil fuels have wreaked havoc on the environment and poisoned the ecology with chemical-laden emissions, as a result, we are turning more and more to RESs, which emit far fewer emissions than fossil fuels. These forms of renewable energy are erratic and unreliable and need to be controlled. Also, the use of EVs is increasing; unquestionably, it will be the driving force metaphorically in the coming decade. If the charge condition of numerous electric vehicles is not correctly controlled, it might have an influence on the quality of the electricity produced.[1] The integration of electric vehicles into the power grid introduces both challenges and opportunities for AGC. [2] Thus, advanced AGC is required for those power systems with RES and EVs. Further research and exploration in that sector are necessary and will be useful to mitigate the frequency regulation problem. [3].

In the power system, the role of AGC is to maintain a balance between the load connected and the power generated, thus maintaining frequency regulation [4,5]. The performance of an automatic generation control system is solely dependent on three factors: 1. the design of the secondary controller and setting the controller's parameters 2. the use of an intelligent optimization algorithm and 3. the performance index that the algorithm employs to assess the fitness of solutions.

Regarding the control approach, conventional controllers such as I, PI, and PID for LFC are still popular with industries because of their simplicity, easy realization, low cost, and robust nature. While they struggle with dynamic or non-linear systems and lack robustness, they also do not adopt advanced control algorithms. Furthermore, different advanced approaches, such as fuzzy logic, Artificial Neural Network based controllers, are designed for AGC [11-13]. While implementing such advanced techniques for frequency regulation, it suffers from different issues. In the case of fuzzy, it is subjectivity in rule definition, difficulty in tuning, challenges in scaling the large and complex system, sensitivity to variation in input data, and limited transparency that make it difficult to interpret the decision-making process. Also, it is a great challenge to acquire accurate, comprehensive knowledge. Regarding the ANN technique, the effectiveness of the controller is highly dependent on the quality of the training data set, and it needs expertise to design because it mainly relies on training data to optimize its parameters. Therefore, the direction that needs to be taken is toward an effective controller that is easy to develop and understand.

Selecting an effective optimization strategy is a basic and crucial difficulty in controller design. Also, Previous studies have demonstrated that choosing the controller parameters is just as important as choosing the type of controller. There are various types of algorithms implemented for frequency control. In [6], the marine predator algorithm is implanted in three different types of systems. Likewise, the authors in [7] used the bird swarm algorithm for multi-area power systems to optimize the gains of the TIDD controller. The article [8] examines the cohort

intelligence optimization (CIO) approach for adjusting the PID controller for load management of a single-area nuclear power station. In [9] the Grey Wolf Optimization-Based Design Margin for a Two-Area LFC Scheme is discussed. Furthermore, a modified African Buffalo optimized dual-stage PI-PDF controller is utilized for multi-microgrid systems [10]. It should be noted that considerable attention has been paid to the application of optimization approaches to aid in the solution of engineering difficulties, particularly the LFC problem. Thus, the choice of algorithm depends on the specific characteristic of the power system and desired performance criteria. This explains the author's decision to use the JAYA method to select the optimal parameters for the suggested DM TD-ID controller in this work.

1.1 Contribution and Paper Organization

Review findings indicate that further investigation is necessary to design an efficient controller tuned with a powerful algorithm that is easy to understand and implement for complex interconnected power systems in order to address the problems with the previously mentioned approaches. Also, the test system so far considered in many articles are of conventional type sources and with less integration of renewable type of source and EVs. To overcome the above-mentioned issues in this paper, a novel DM TD-ID controller is proposed. This proposed controller uses the dual mode scheme, which switches between the integral derivative mode and tilt derivative mode. This proposed DM TD-ID controller operates effectively, has an easy-to-understand structure, and is simple in its operation. Furthermore, a simple reliable JAYA algorithm is used to optimize the proposed controller gains. The proposed controller is implemented in the realistic test system consist different power generations and EVs in each area of the system. The forthcoming work is organized as follows. Section 2 delves into the objectives and goals of the proposed work, while Section 3 explains the mathematical modelling of the TAHPS. Next to that Section 4 presents the suggested controller design and its implementation. In Section 5, the problem formulation and the JAYA algorithm's operation are covered. And finally, Section 6 concludes with a presentation of the proposed work's conclusion and its future scope. It also presents the simulation results of the planned effort. All the major objectives of the paper are be pointed as follows

- To design a new and robust DM TD-ID controller for the realistic TAIPS.
- To model a realistic test system which is a three-area interconnected power system (TAIPS) by considering the effects of RESs of wind power and solar PV. Also, to integrate the EV in each area of the TAIPS in MATLAB Simulink platform.
- To simulate the modelled TAIPS with the proposed DM TD-ID controller for 1% of step load perturbation (SLP) to tune the controller parameters with a simple and efficient JAYA algorithm, and to reveal the benefits by comparing it with other bench-mark controllers.
- To perform sensitivity and performance analyses in order to show the proposed controller's efficacy under different scenarios.

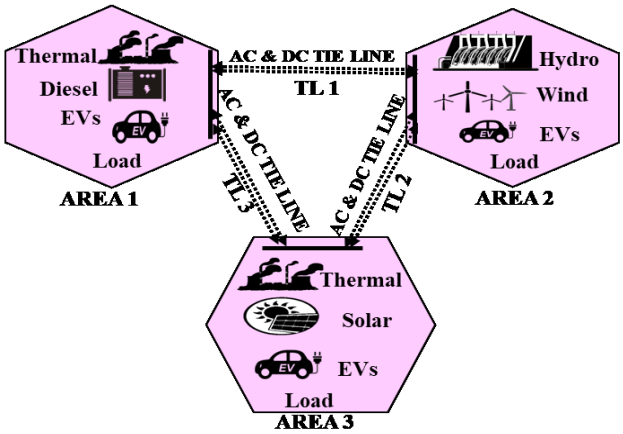


Fig. 1. Three area hybrid system one-line diagram.

2. Test System

Simulating realistic systems allows researchers and engineers to capture the intricacies of power generation, transmission, and distribution, including the effects of various disturbances and uncertainties. Thus, in this paper a complex realistic three area power system (TAIPS) encompasses conventional, non-conventional and group of EVs. The Fig. 1 is displaying the one-line diagram of the TAIPS under consideration. As said before in this TAIPS, the load, the group of EVs, and two distinct types of generation sources are present in each area.

The thermal power plant, the diesel plant, the group of 100 EVs, and the load are all located in area 1. Also, area 2 has group of 100 EVs and load connections in combination to generations of hydro and wind power plants. Lastly, area 3 includes a thermal power plant, solar PV, a group of 100 EVs, and load. Each area is connected to other area by AC as well as DC tie-lines. The Mathematical modelling of each system is described below. [14-15],27. The modelling of thermal plant is given in Eq (1)-(3). Where K_{Ti} is the gain constant and Ti is the time constant of the thermal powerplant

- Thermal power plant

$$\Delta G_{TH1} = K_{T1}/ (T_{T1} S) +1 \quad (1)$$

$$\Delta G_{TH2} = (K_{T2}*T_{T2} S+1)/ (T_{T2} S) \quad (2)$$

$$\Delta G_T_{H3} = K_{T3}/ (T_{T3} S) +1 \quad (3)$$

$$\Delta G_{PS} = K_{PS}/ (T_{PS} S)+1 \quad (4)$$

Where in Eq (4), represents the power system in each area.

- Hydropower plant

$$\Delta G_{HY1} = (K_{H1}/ (T_{H1} S+1))*((T_{H11} S+1)/(T_{H12} S+1)) \quad (5)$$

$$\Delta G_{HY2} = (—(T_{H2}+1) / (0.5*T_{H2} S+1)) \quad (6)$$

In equations (5)-(6), the hydro governor gain and time constant are denoted by K_{H1} and T_{H1}. While, T_{H11} and T_{H12} represent the hydro governor's rising time, transient droop, and nominal flow times, respectively.

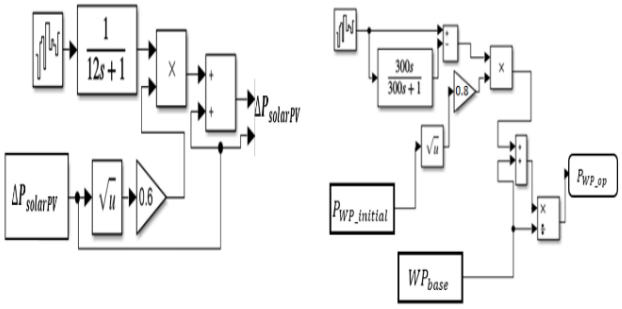


Fig. 2. Varying solar and wind power model.

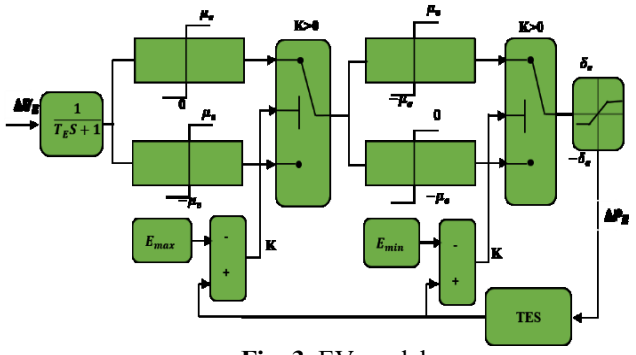


Fig. 3. EV model

➢ HVDC (High Voltage Direct Current) system.

The HVDC lines can be included along with the AC tie-lines to boost the tie-line power transmission capacity. The converter-inverter section built within the HVDC line is operated according to the pertinent switching strategy. The transfer function to represent the HVDC line is given in Eq (7).

$$\Delta P_{DC}=K_{DC}/ (1+T_{DC}) \quad (7)$$

➢ Solar PV plant and Wind power plant

In order to contemplate real time situation a dynamic wind and solar power is modelled here. The variance between uniform and non-uniform insolation and wind speed may be used to calculate the power fluctuations of the solar PV and wind generation system in this model. According to various LFC research, including the random output fluctuation that can be created by the white noise block is magnified by the standard deviation to produce the output power fluctuation of the PV system and wind power as shown in Fig.2. It has been suggested that the following function might simulate the PV power variance and wind power variance to replicate the actual shift in generated powers. Its equation is given by Eq (8) and (9) [16-17].

$$\Delta P_{solarPV} = 0.6\sqrt{P_{solarPV}} \quad (8)$$

$$\Delta P_{wp} = 0.8\sqrt{P_{wp_op}} \quad (9)$$

➢ Electrical Vehicle

The corresponding model that will ultimately be utilized for AGC is shown in Fig. 3. It makes an effort to simulate the actions of a single EV battery. The total power required to charge or discharge an electric vehicle may be determined using this EV model. In Fig.3, the AGC signal is represented by U_E, and T_E stands for the EV's time constant [18]. Additionally, the inverter capacity and power ramp rate restrictions are denoted by the ±μe and ±δ respectively. E_{max} and E_{min} stand for the maximum and minimum controlled energies of the battery, respectively, where E represents the energy of the EV battery. The charging/discharging power is

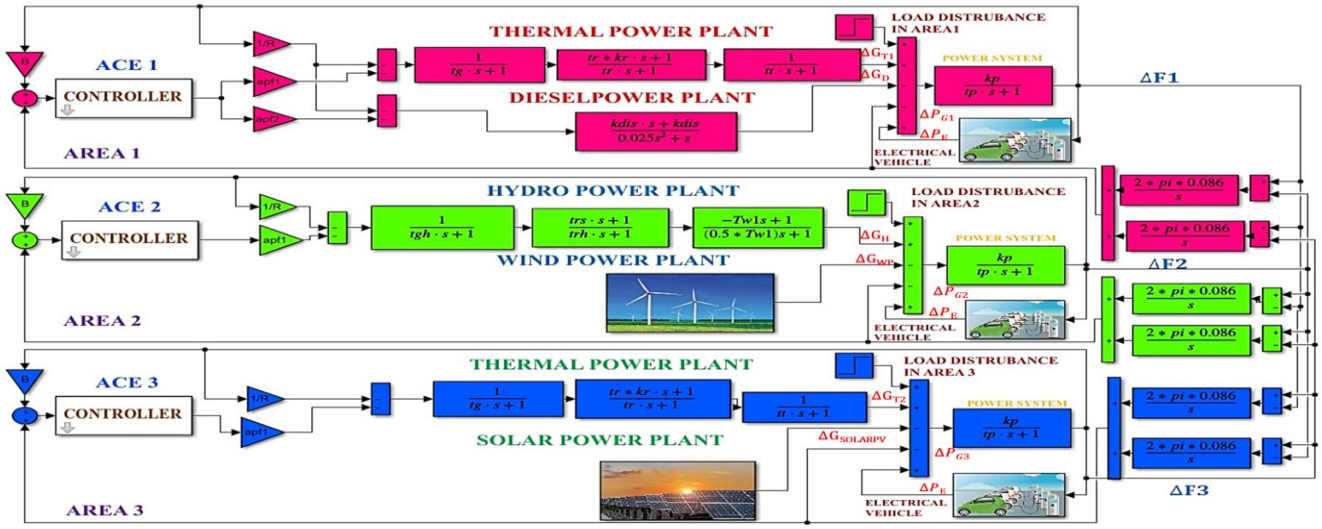


Fig. 4. Transfer function Model of three area interconnected power system (TAIPS).

displayed by ΔP_E. The EV is considered to be in the idle state when $\Delta P_E = 0$, whereas $\Delta P_E > 0$ specifies that the EV is discharging and $\Delta P_E = 0$ shows that the EV is charging. The boundaries for charging and discharging EVs are represented by $\pm\mu_e$. It should be remembered that an EV can only be discharged within the range of 0 to μ_e since it can no longer be charged once its stored energy surpasses the upper limit Emax. The EV can only be charged within the range of ($-\mu_e \sim 0$) if the stored energy is less than the lower limit E_{min} [1,19]. The final transfer function model of TAIPS composed of different generation sources and EVs modelled in Simulink platform is presented in fig.4.

3. Controller Design

This section provides detailed information on design of the controller. Given that I, PI, PID control is the popular and well-known conventional control approach for LFC problems, this study will not explore the structure or transfer function of a such controllers. Thus, following that in this research work a unique controller named Dual mode Tilt derivative -integral derivative controller (DM TD-ID) is designed for the first time. A detailed explanation is provided in the ensuing section.

3.1 TID Controller Design

When compared to a conventional PID controller, the tilt controller (T) provides simpler tuning, a greater ratio of disturbance rejection, and less effects of plant parameter fluctuations on closed loop response. Similar in structure to a PID control, a TID control substitutes a transfer function block denoted by (1/S^(1/n)) for the proportional control block in a PID control. Its name is termed as "Tilt" controller for this transfer function block [20]. The structure and controller action of TID controller is given in the Fig. 5.

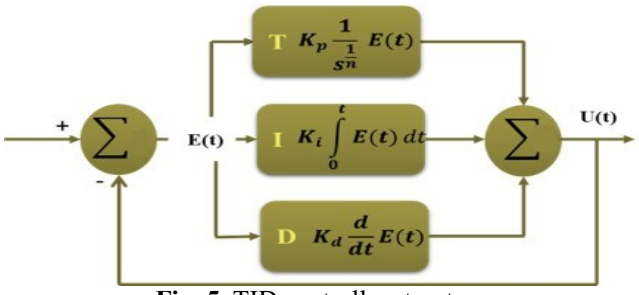


Fig. 5. TID controller structure.

3.2 The Dual Mode Scheme

When considering other complex control strategies, the dual-mode approach is more time-efficient and easier to understand during the implementation phase and more effective than conventional methods [21]. A well-tuned P or I controller may accomplish zero error in steady state, but because of the large overshoot and undershoot, the system takes longer to respond and makes up for lost time. This paradox can be resolved by applying the idea of a dual-mode scheme. Using a dual-mode switch (let mode a mode b), one controller at a time is connected to the feedback loop in this method.

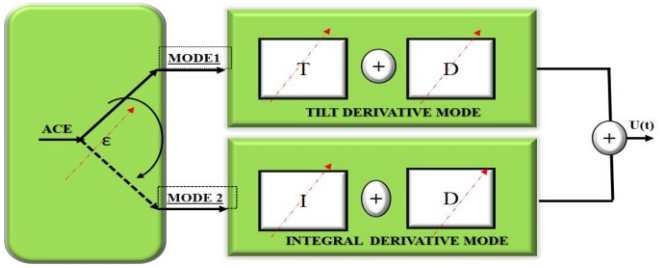


Fig. 6. The proposed DM TD-ID controller structure.

In simple words, when the error is large, then mode A is activated and for minimized error mode B is activated. By considering its simple and efficient working, it is incorporated in the proposed controller structure. This paradox can be resolved by applying the idea of a dual-mode scheme. Using a dual-mode switch (let mode a mode b), one controller at a time is connected to the feedback loop in this method. In simple words, when the error is large, then mode A is activated and for minimized error mode B is activated. By considering its simple and efficient working, it is incorporated in the proposed controller structure.

3.3 The Proposed DM TD-ID Controller Structure

In the proposed control technique, the dual mode scheme is utilized by considering two modes of TD and ID. The control structure of DM TD-ID controller is shown in the Fig. 6. In this it will act in two modes of operation according to the error signal E(t) [22]. The TD controller combines the action of tilt controller and derivative controller. The tilt (T) controller will reduce the disturbance (i.e. steady state error) in a fast way whereas in the ID control mode the integral and derivative action is combined. On that the integral(I) controller reduces the error near to zero. Given the complexity of the system under consideration, the derivative controller is provided in both modes to reduce overshoot and enhance transient response.

In the controller action equation 10,11, the difference between scheduled and actual value of frequency is termed as area control error (ACE) which is considered as E(t). Following that the non-zero value is utilized as switching limit ε. The switching limit ε is chosen after a numerous simulation of the TAIPS system under uncontrolled case and with tilt derivative controller alone [23]. And U(t) is output signal to the plant and E(t) is the input signal to the controller.

3.4 Operation of Proposed Controller

The control action equations (10,11) make it simple to understand how the controller work in simple way. When the E(t) is larger than the switching limit ε then the TD control mode is activated to reduce steady state error faster manner as in equation 10. For trivial range of error signal E(t) according to equation 11 ID mode is activated as it tries to bring the error back to setpoint. Consequently, the controller operates in this way and works on errors signal.

$$U(t) = K_p \frac{1}{S\bar{n}} E(t) + K_d S\, E(t) \quad \text{for ACE} > \varepsilon \tag{10}$$

$$U(t) = \frac{K_i}{S} E(t) + K_d S\, E(t) \text{ for ACE} \leq \varepsilon \tag{11}$$

4. Problem Formulation and JAYA Algorithm

In this section, the problem formulation and the algorithm implemented are discussed in detail.

4.1 Problem Formulation

The performance index Integral Square Error (ISE) is incorporated as objective function J for the load frequency control is presented in the equations (12) and (13). Where, β is the biasing coefficient, ΔF_i is the deviation of frequency in i^{th} area and $\Delta P_{tie\ ij}$ is the change of tie-line power and subject to constraints of minimum and maximum value of control variables.

$$E(t) = ACE = \beta_i \Delta F_i + \Delta P_{tie\text{-}ij} \tag{12}$$

$$Min\ J = \int_0^t E(t)^2 dt \tag{13}$$

Subject to constraints

$K_{tmin} \leq K_t \leq K_{tmax}$
$n_{min} \leq n \leq n_{max}$
$K_{imin} \leq K_i \leq K_{imax}$
$K_{dmin} \leq K_d \leq K_{dmax}$
$\varepsilon_{min} \leq \varepsilon\ i \leq \varepsilon_{max}$

The simple and efficient JAYA algorithm is implemented for effective tuning of the controllers considered in this research work, which include I, PI, PID, TID, and the proposed DM TD-ID controller.

4.2 Jaya Algorithm

As said before, the significant and simple JAYA algorithm is utilized to obtain the controller values. This method is population-based and has few processes, making it simple to understand. The algorithm constantly seeks to move closer to success (i.e., finding the ideal answer) and seeks to prevent failure (i.e., moving away from the worst answer). The algorithm, which goes by the name JAYA (Victory), aims to prevail by finding the best. The proper tuning of algorithm-specific parameters as well as the tuning of common governing parameters is necessary for all evolutionary and swarm intelligence-based algorithms [24]. The efficiency of the algorithm can fluctuate depending on how the tuning of its particular parameters is done. It has some control parameters. The value used are population size of 30 and the number of generations of 50. Contrary to other algorithms, JAYA does not have any specific parameters. The best outcome of the JAYA algorithm can be obtained, though, even without using any specific settings. The Fig. 7 is the flow chart of JAYA algorithm. For minimization problem, $f(x)_{new} < f(x)_{old}$ is update condition. Likewise, for maximization problem, $f(x)_{old} < f(x)_{new}$ is update condition.

$$X_{p,q,t}^{new} = X_{p,q,i} + r_{1,p,q}\left(X_{p,best,i} - \left|X_{p,q,i}\right|\right) - r_{2,p,q}\left(X_{p,worst,i} - \left|X_{p,q,i}\right|\right) \tag{14}$$

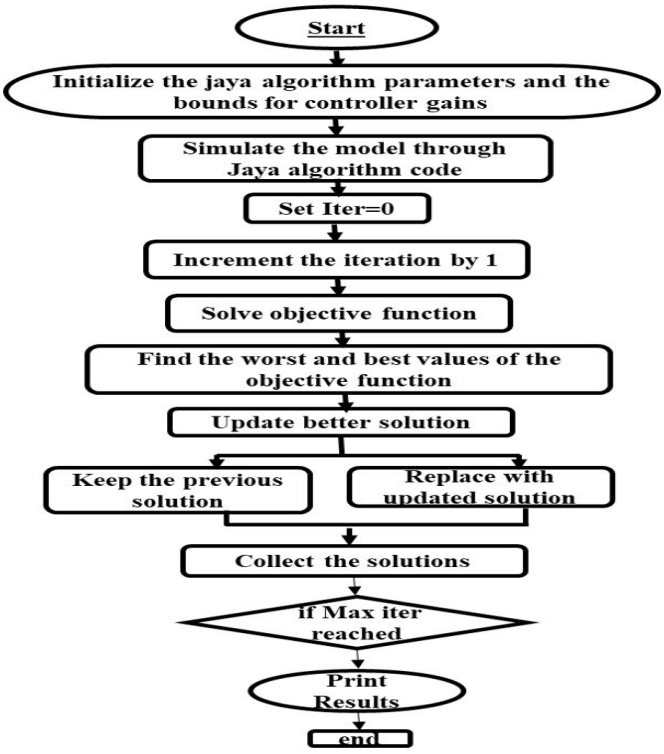


Fig. 7. The Flow chart of JAYA algorithm.

Likewise, for maximization problem, $f(x)_{old} < f(x)_{new}$ is update condition. where $X_{p,q,i}$ is the p^{th} variable's value for the q^{th} candidate during the ith iteration, the value is modified in accordance with the Eq. (14). Here, $r_{2,p,q}$ and $r_{1,p,q}$ are the random value range between [0,1]. $X_{p,q,t}^{new}$ is the updated $X_{p,q,i}$. And the term $r_{1,p,q}(X_{(p,best,i)} - |X_{p,q,i}|)$ is the tendency of the solution to approach the ideal solution and $-r_{(2,p,q)}(X_{(p,worst,i)} - |X_{p,q,i}|)$ is propensity to steer clear of the worst option [25-26].

Pseudo code for JAYA Algorithm

Initialize Population size, no of variables, stopping factor
While stopping factor not attained do
Evaluate the best and
Modify the solution with equation (14)
Update the prior solution
Until n update in previous one
Output the optimized solution.

4.3 Algorithm Implementation to the proposed controller

The boundaries of the variables that need to be adjusted are given to the algorithm as inputs, which is coded on the MATLAB platform. For each iteration the algorithm will give set.

In this case, achieving the maximal number of iterations will yield the optimal variable values by simulating the transfer function with the variables for each iteration and reducing the cost function, which will minimize the error by minimizing the performance index. The algorithm is covered in more detail in the section.4.2.

5. Results and Discussion

Along with other controllers of I, PI, PID, and TID, the proposed DM TD-ID controller is implemented in the TAIPS for 1% of SLP in each area. A highly effective and uncomplicated JAYA algorithm is used to tune the controller parameters during simulation.Using the MATLAB Simulink platform, a proposed JAYA optimized DM TD-ID controller is simulated in each area of the TAIPS's transfer function model for 1200 seconds which is depicted in Fig. 4. The obtained graphical outputs are represented in Fig. 8(a)–8(f). And the corresponding change in frequency of each area, tie-line power and performance index obtained are presented in the Table 1. Decrement of system Performance Index(J) leads to easier and better control system stability [28]. From the computed Performance Index(J) value given in Table 1, it is evident that the proposed DMTD-ID controller structure has the minimal Performance Index(J) value of 0.16 than others and also shows which proves the stability of the proposed controller structure. From the output, it is visible that the. proposed controller shows less deviation than other bench mark controllers output for the simulation timeof 1200secs. The test system is simulated for 60 seconds in order to compare the performance indices, and the related performance indices for undershoot, overshoot, and settling time of frequency deviation in area1, area2, area3 and one tile-line waveforms were reported in Table 2.

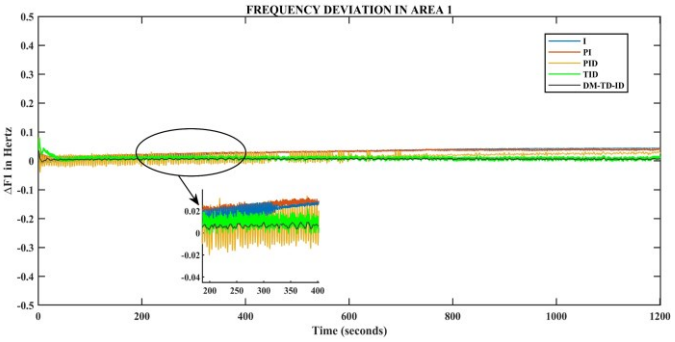
Table 1. Numerical output of different controllers frequency change and tie-line power change and performance index

Controller	I	PI	PID	TID	DM TD-ID
ΔF_1 in Hz	0.044	0.042	0.025	0.005	**0.005**
ΔF_2 in Hz	-0.02	-0.044	0.025	0.057	**0.004**
ΔF_3 in Hz	0.085	0.113	0.014	0.017	**0.003**
ΔT_1in pu (-)	0.045	0.048	0.099	0.019	**0.013**
ΔT_2 in pu	-0.07	-0.070	0.024	0.069	**0.016**
ΔT_3 in pu	0.118	0.119	0.074	-0.017	**-0.002**
J(Performance Index)	33.95	45.23	2.38	2.58	**0.16**

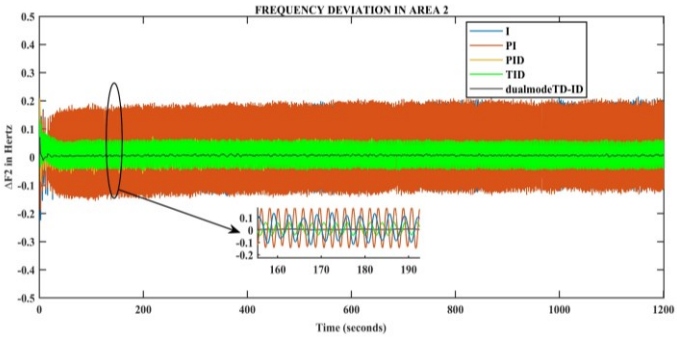
From the results obtained, it is evident that for the TAIPS along with the RES and EVs, the proposed DM TD-ID controller outperforms other benchmark controllers of I, PI, PID, and TID controller even in the presence of varying RES, the proposed DM TD-ID controller shows very little variation in frequency deviation in all areas and in the tie-line powers. Also, efficacy of the suggested control mechanism is assessed for the TAIPS in this section using different scenarios and the results are discussed as follows.

Table 2. .Numerical output of performance Indices

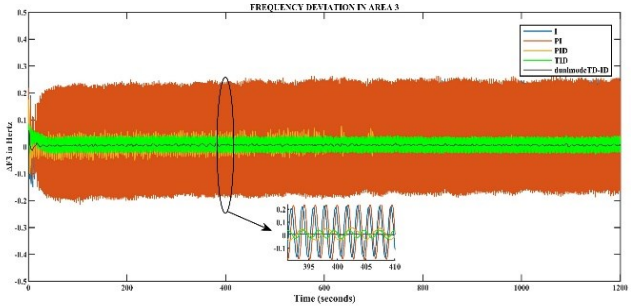
Area	Controller	Us	Os	Ts in secs
1	I	-0.01	0.016	10
	PI	-0.004	0.03	30
	PID	-0.04	0.082	12
	TID	-0.008	0.009	10
	DM TD-ID	-0.003	0.03	6
2	I	0.2	0.21	12
	PI	0.18	0.2	30
	PID	0.08	0.21	14
	TID	0.12	0.132	8
	DM TD-ID	0.011	0.071	5
3	I	0.121	0.212	10
	PI	0.195	0.214	50
	PID	0.09	0.17	10
	TID	0.148	0.071	9
	DM TD-ID	0.013	0.06	5
Tie-Line	I	0.03	0.17	40
	PI	0.03	0.109	40
	PID	0.06	0.081	12
	TID	0.05	0.072	7
	DM TD-ID	0.01	0.0298	5



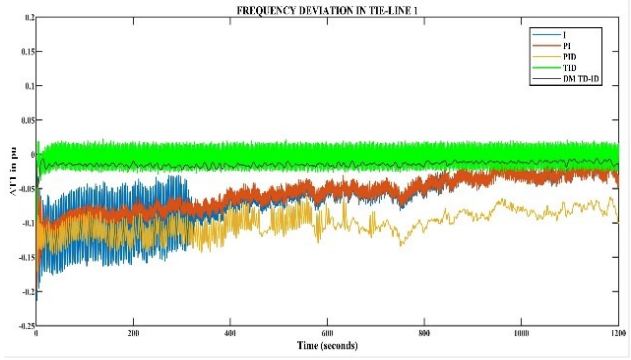
(a)



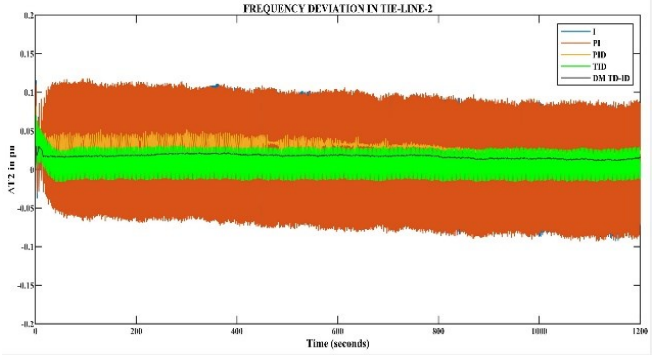
(b)



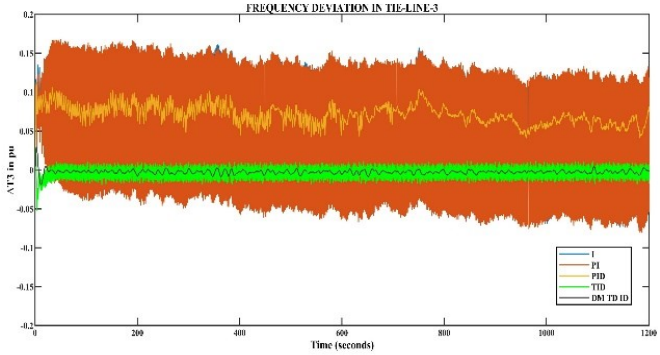
(c)



(d)



(e)

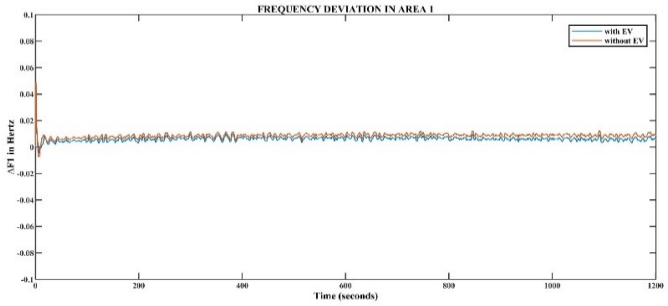


(f)

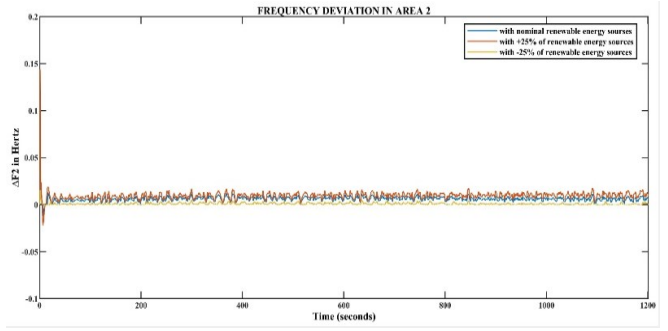
Fig. 8. Frequency deviation in(a) area1(b) area2 (c)area3(d) Tiel-ine1(e) Tie-line2 (f) Tie-line3.

5.1 Scenario:1 System performance in the presence and absence of EV

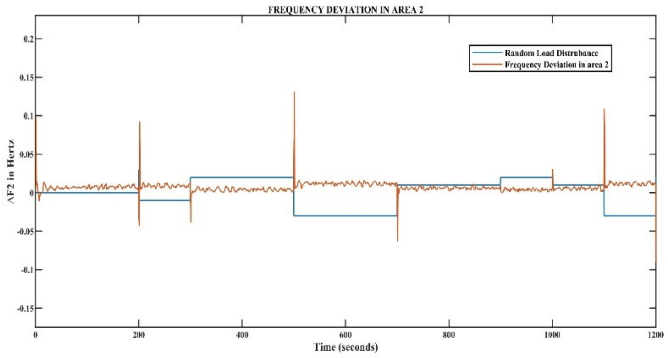
In order to confirm that the controller functions both with and without the EVs, a simulated TAIPS is carried out. The TAIPS is simulated in both the presence and absence of the EVs. For simplicity the output from area 1 is represented for verification. The corresponding output is shown in the Fig. 9(a). It shows that the presence of EVs or absence of EV doesn't affect the controller efficient working. In both the cases the proposed DM TD-ID controller performs well as it shows very minimum deviation.



(a)



(b)

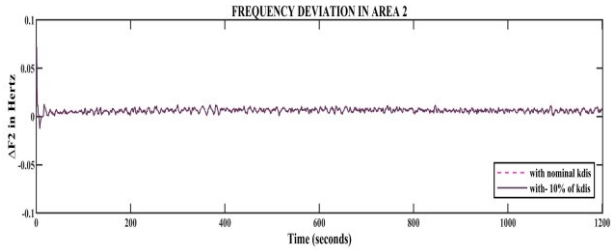


(c)

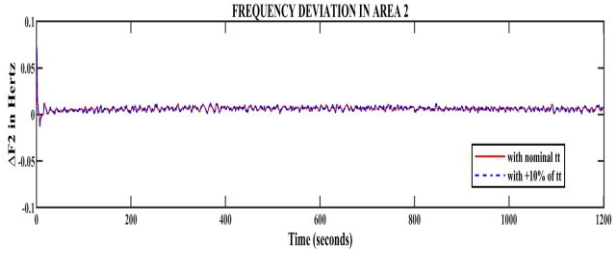
Fig .9. Frequency Deviation in area 2 for (a) Scenario 1 (b) Scenario 2 (c)Scenario 3.

5.2 Scenario:2 System performance under different operating conditions of renewable energy sources

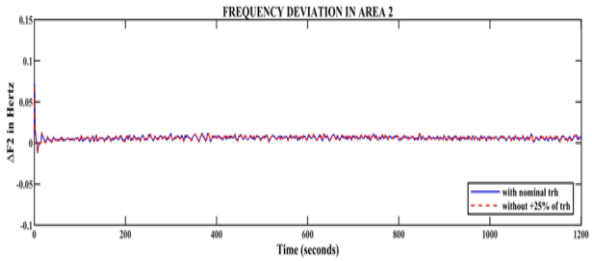
In this section the input to the TAIPS is varied with solar insolation rate and wind speed by +25% and -25% and the output from area 2 is shown in the Fig 9(b). It shows that the proposed controller strategy worked effortfully even in the case of increased or decreased number of renewables with less deflections in waveforms.



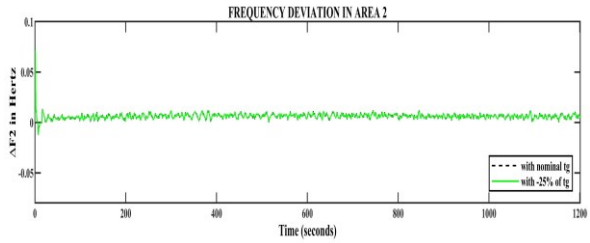
(a)



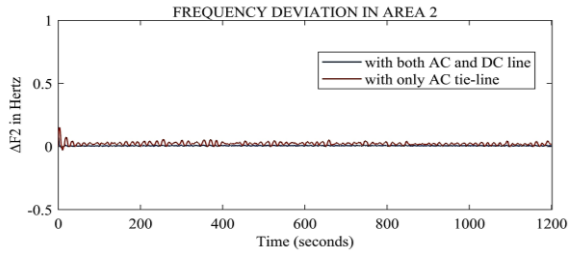
(b)



(c)



(d)



(e)

Fig .10. (a)-(d) Frequency Deviation in area 2 for Scenario 4, (e) Frequency Deviation in area 2 for Scenario 5

5.3 Scenario:3 Performance Analysis with random load pattern

To scrutinize the performance of the proposed controller in the TAIPS, the randomly varying load is given for 1200 secs and the respective output is depicted in the below Fig. 9(c) for area 2. The resultant waveforms for sudden varying load become stable system within small duration after the sudden change occurs. It shows that the proposed controller is robust for varying load pattern.

5.4 Scenario:4 Sensitivity Analysis with parameter variation

In this scenario, the gain constant of the diesel plant, the time constant of the thermal plant's turbine in area 3, the hydro plant's reheat turbine time constant, and the governor time constant of area1 are all varied for between ±10% and ±25% and the results of the sensitivity analysis for the TAIPS are obtained and depicted in Figs 10(a)-(d). Only area 2's output is shown here. The results prove that the proposed controller is less sensitive to system parameter variations.

5.5 Scenario:5 Simulation results with only AC tie line

Both the AC and DC tie-lines are used in this study. Because both AC and DC tie-lines combine the benefits of different transmission systems for an integrated power system with a range of RESs and EVs, they increase the sustainability of the system. The system is simulated using only an AC tie-line in order to understand how the suggested controller for the system would function in this scenario. The results are shown in Figure 10(e). It is evident from the results that there were very few variances in the system performance. Therefore, the proposed controller is better suited for power systems that simply have an AC tie-line. Thus, the presence of parallel AC-DC line improves the reliability and sustainability of the TAIPS.

6. Conclusion and Future Scope

In this research work, a novel, reliable DM TD-ID controller is successfully proposed and implemented for the test system for 1% of step load perturbation. A simple and efficient JAYA algorithm is employed to obtain the controller gains and accordingly, the authors conclude with the following words:

- For the test system, which consists of a three-area integrated power system with different generation sources along with dynamic RES and EVs in each area, the JAYA-optimized DM TD-ID controller is implemented and verified to have a performance index (ISE) of 0.16, which is very small compared to other controllers.
- The change in tie-line power waveform and frequency deviation waveforms were evaluated for the settling time, overshoot, and undershoot performance indicators. The result shows that the proposed DM TD-ID controller for the test system performs better in the performance indices and shows less volatility than other controller types.
- When EVs are present or absent, the suggested DM TD-ID controller operates admirably because it exhibits very little variance. Additionally, the suggested controller technique performed well, even with a change in the quantity of renewable energy sources and minimal waveform deflections. It demonstrates how resilient the DM TD-ID controller is to changing load patterns.

- The outcomes of the sensitivity analysis demonstrate how less susceptible the proposed controller is to changes in system parameters. The results clearly show that there were not many variations in the system's performance.
- The system performance in the presence and absence of a HVDC tie-line also performed. As such, power systems with only an AC tie-line are also better suited for the proposed controller. From the results the proposed DM TD-ID controller is proved to be superior to other compared controllers by providing stable output than others.

Overall, from the comparison of results, it is evident that the DM TD-ID controller outperforms other controllers successfully with minimum variation. And also, different scenarios, which include sensitivity analysis and performance analysis, prove the robustness of the controller and its superiority over the other controllers. Further the proposed controller can be applied to other power system models with different combination of energy sources and their effects may be studied along with energy storage devices.

Conflicts of Interest

The authors declare that there is no conflict of interests regarding the publication of this paper.

Acknowledgements

The authors thank the Department of science and technology (DST), New Delhi for having provided the necessary facilities through the FIST-level l program in the Energy Conversion Lab attached to the Department of ElectricalEngineering at Annamalai University, to carry out the work relating to the area under study.

Appendix 1

In TAIPS [19], [21-22]. Diesel plant: K_{DIS}=16.50, Hydro plant:T_{H1}=48.7 s; T_{H11}=0.513 s; H_{12}=10s; T_{H2}=1s .Wind plant: K_{W1}=1.25; T_{W1}=0.6; K_{W2}=1.4; T_{W2}=0.041s ,Hydro plant:T_{H1}=48.7 s; T_{H11}=0.513 s; T_{H12}=10s; T_{H2}=1s.,Solar plant: K_{P1}= -18 T_{P2}=100s; K_{P2}=900; T_{P2}=50 s. Thermal plant: apf1=0.65 apf2=0.35, B=0.425 Hz/pu MW; T_{T1}=0.08s; T_{T2}=10s; K_{T2}=0.3 Hz/pu MW; T_{T3} =0.3s. K_{PS}= 120 Hz/pu MW; T_{PS}=20 s; R=2.4 puMW/Hz.

Appendix 2

In EVs [17] T_{E1}= 1s; δ_E = 2 0.01 pu MW/s; μ_E= 0.016 pu MW; E_{max}= 0.9 pu MWh; E_{min}= 0.8 pu MWh.

References

[1] K. Ullah, A. Basit, Z. Ullah, F. R. Albogamy and G. Hafeez, “Automatic generation control in modern power systems with wind power and electric vehicles”, Energies, MDPI, DOI:10.3390/en15051771, Vol.15, No.5, pp.1771,2022.

[2] A. Kilic, “Analysis of charging systems for electric vehicle”, International Journal of Smart Grid, DOI:10.20508/ijsmartgrid.v7i4, Vol.7, No.3, pp.168-177, 2023.

[3] Y. Arya, “Effect of electric vehicles on load frequency control in interconnected thermal and hydrothermal power systems utilizing CF-FOIDF controller”, IET Generation, Transmission & Distribution, IET, DOI: 10.1049/iet-gtd.2019.1217, Vol. 14, No. 14, pp. 2666-2675, 2020.

[4] M. M. Gulzar, S. Murawwat, D. Sibtain, K. Shahid, I. Javed and Y. Gui, “Modified cascaded controller design constructed on fractional operator ‘β’to mitigate frequency fluctuations for sustainable operation of power systems”, Energies, MDPI, DOI: 10.3390/en15207814, Vol.15, No.20, pp.7814, 2022.

[5] D. Mishra, M.K. Maharana, M.K. Kar, and A. Nayak, “Frequency management of an interconnected power system using modified differential evolution algorithm”, International Journal of Renewable Energy Resources, Gazi University, DOI: 10.20508/ijrer. v13i2.13555.g8772, Vol.13 No.2, pp.515-525,2023.

[6] Halmous, Y. Oubbati, M. Lahdeb and S. Arif, “Design a new cascade controller PD-P-PID optimized by marine predators algorithm for load frequency control”, Soft Computing, Springer, DOI: 10.1007/s00500-023-08089-w, Vol.27, No.14, pp. 9551-9564,2023.

[7] S. K. Bhagat, S. Behera, A. Saha, T. Bal, T. Chiranjeevi, R. Devarapalli and N. R. Babu, “Bird swarm algorithm optimized TIDD controller for multi-area load frequency control application”, SN Computer Science”, Springer, DOI: 10.1007/s42979-022-01556-5, Vol.4, No.2, pp. 138, 2023.

[8] D. Murugesan, K. Jagatheesan, A.J. Kulkarni and P. Shah, “A socio inspired technique in nuclear power plant for load frequency control by using cohort intelligence optimization-based PID controller”, In Renewable Energy Optimization, Planning and Control: Proc. of ICRTE, Springer Nature, Singapore, pp. 1-12, 2022.

[9] M. H. Ibrahim, A. S. Peng, M. N. Dani, A. Khalil, K. H. Law, S. Yunus and T. W. Au, “A novel computation of delay margin based on grey wolf optimization for a load frequency control of two-area-network power systems”, Energies, MDPI, DOI: 10.3390/en16062860, Vol. 16, No. 6, pp. 2860, 2023.

[10] B. Singh, S. K. Bishnoi, M. Sharma, P. Singh, and S. Dhundhara, “An application of nature inspired algorithm based dual-stage frequency control strategy for multi micro-grid system”, Ain Shams Engineering Journal, Science Direct, DOI: 10.1016/j.asej.2023.102125, Vol. 14, No. 9, pp.102125, 2023.

[11] M. Kendzi and, A. Aissaoui, "Comparison between the mit rule and fuzzy logic controller to adapting the power generated by a doubly fed induction generator integrated in a wind system”, 10th International

Conference on Smart Grid, Istanbul, Turkey, pp. 231-235, 27-29 June 2022.

[12] M. Colak, I. Cetinbas and, M. Demirtas, "Fuzzy logic and artificial neural network based grid-interactive systems for renewable energy sources: A review" , 9th International Conference on Smart Grid, Setubal, Portugal, pp. 186-19, 29 June-1 July 2021.

[13] A. Benyounes, A. Iratni, A. Hafaifa, and I. Colak, "A comparative modeling study of gas turbine using adaptive neural network nonlinear autoregressive exogenous, and fuzzy logic approaches for modeling and control", International Journal of Smart Grid, DOI:10.20508/ijsmartgrid.v7i2.288.g275, Vol.7, No.2, pp.90-102,2023.

[14] S. A. Pavadaisami, M. T. A. Musthafa and V. K. N. Jeganathan, "Automatic generation control of three area hybrid power system by sine cosine optimized dual mode fractional order controller", International Journal of Renewable Energy Research, Gazi University, DOI: 10.20508/ijrer. v12i3.13127.g8524, Vol.12, No.3, pp.1414-1426, 2022.

[15] H. H. Ali, A. Fathy and A. M. Kassem, "Optimal model predictive control for LFC of multi-interconnected plants comprising renewable energy sources based on recent sooty terns approach," Sustainable Energy Technologies and Assessments, Science Direct, DOI: 10.1016/j.seta.2020, Vol. 42, pp. 100844, December 2020.

[16] E.M. Ahmed, E. A. Mohamed, A. Selim, M. Aly, A. Alsadi, W. Alhosaini and H. A. Ramadan, "Improving load frequency control performance in interconnected power systems with a new optimal high degree of freedom cascaded FOTPID-TIDF controller", Ain Shams Engineering Journal, Science Direct, DOI: 10.1016/j.asej.2023.102207, Vol. 14, No. 10, pp. 102207, 2023.

[17] D.C. Das, A.K Roy, and N. Sinha, "GA based frequency controller for solar thermal–diesel–wind hybrid energy generation/energy storage system", International Journal of Electrical Power & Energy Systems, Science Direct, DOI: 10.1016/j.ijepes.2012.05.025, Vol.43, No. (1), pp.262-279,2012.

[18] M.H. Khooban, T. Niknam, F. Blaabjerg and T. Dragičević, "A new load frequency control strategy for micro-grids with considering electrical vehicles", Electric Power Systems Research, Science Direct, DOI: 10.1016/j.epsr.2016.10.057 Vol.143, pp.585-598,2017.

[19] S. Mandal, "An analysis of braking energy regeneration in electric vehicles" International Journal of Renewable Energy Research, Gazi University, DOI: 10.20508/ijrer. v7i3.5770.g7130, Vol.7, No.3, pp.999-1006,2017.

[20] M. Ahmed, G. Magdy, M. Khamies, S. Kamel, "Modified TID controller for load frequency control of a two-area interconnected diverse-unit power system", International Journal of Electrical Power & Energy Systems, Science Direct, DOI: 10.1016/j.ijepes.2021.107528, Vol.135, pp.107528, 2022.

[21] S. A. Pavadaisami, M. T. A. Musthafa and V. K. N. Jeganathan, "Particle swarm optimization based dual-mode fractional order control for automatic generation control of two area interconnected hybrid system", International Journal of Intelligent Engineering & Systems, INASS, DOI: 10.22266/ijies2022.0831.09, Vol. 15, No.4, pp.86-96, 2022.

[22] M. R. Sathya and M. Mohamed Thameem Ansari, "Design of biogeography optimization based dual mode gain scheduling of fractional order PI load frequency controllers for multi source interconnected power systems", International Journal of Electrical Power and Energy Systems, DOI: 10.1016/j.ijepes.2016.04.006, Vol. 83, pp. 364–381, December 2016.

[23] S. Velusami and I.A. Chidambaram, "Decentralized biased dual mode controllers for load frequency control of interconnected power systems considering GDB and GRC non-linearities", Energy Conversion and Management, DOI: 10.1016/j.enconman.2006.11.003, Vol.48, pp.1691–1702, December 2006.

[24] R. Rao, "Jaya: A simple and new optimization algorithm for solving constrained and unconstrained optimization problems", International Journal of Industrial Engineering Computations, Growing Science, DOI: 10.5267/j.ijiec.2015.8.004, Vol.7 No.1, pp.19-34, 2016.

[25] S. Bhongade, VP. Paramar, "Automatic generation control of two-area ST-Thermal power system using jaya algorithm", International Journal of Smart Grid, DOI: 20508/ijsmartgrid.v2i2.20.g20, Vol.2, No.2, pp.99-110,2018.

[26] S. Pahadasingh. C. Jena, C. K. Panigrahi and B. P. Ganthia, "JAYA algorithm-optimized load frequency control of a four-area interconnected power system tuning using PID controller", Engineering, Technology & Applied Science Research, DOI:10.48084/etasr.4891, Vol.12, No.3, pp.8646-8651, 2022.

[27] S. Kumari, G. Shankar ," Maiden application of cascade tilt-integral–tilt-derivative controller for performance analysis of load frequency control of interconnected multi-source power system", IET Generation, Transmission & Distribution. DOI:10.1049/iet-gtd.2018.6726, Vol. 13, No.23, pp. 5326-38, December 2019.

[28] O. Atayeb, M. Muawia, "Robust PID control system design using ITAE performance index (DC Motor Model)", International Journal of Innovative Research in Science, Engineering and Technology, pp. 2319-8753, 2014.